

Review

Open Access



A mini review of machine learning in inorganic phosphors

Lipeng Jiang¹, Xue Jiang¹, Guocai Lv², Yanjing Su^{1,*}

¹Beijing Advanced Innovation Center for Materials Genome Engineering, Corrosion and Protection Center, University of Science and Technology Beijing, Beijing 100083, China.

²Basic Experimental Center of Natural Science, University of Science and Technology Beijing, Beijing 100083, China.

*Correspondence to: Prof./Dr. Yanjing Su, Beijing Advanced Innovation Center for Materials Genome Engineering, Corrosion and Protection Center, University of Science and Technology Beijing, 30 Xueyuan Road, Beijing 100083, China. E-mail: yjsu@ustb.edu.cn

How to cite this article: Jiang L, Jiang X, Lv G, Su Y. A mini review of machine learning in inorganic phosphors. *J Mater Inf* 2022;2:14. <https://dx.doi.org/10.20517/jmi.2022.21>

Received: 19 Jul 2022 **First Decision:** 15 Aug 2022 **Revised:** 2 Sep 2022 **Accepted:** 9 Sep 2022 **Published:** 16 Sep 2022

Academic Editor: Xingjun Liu **Copy Editor:** Jia-Xin Zhang **Production Editor:** Jia-Xin Zhang

Abstract

Machine learning has promoted the rapid development of materials science. In this review, we provide an overview of recent advances in machine learning for inorganic phosphors. We take two aspects of material properties prediction and optimization based on iterative experiments as entry points to outline the applications of machine learning for inorganic phosphors in terms of Debye temperature prediction and luminescence intensity and thermal stability optimization. By analyzing the machine learning methods and their application objectives, current problems are summarized and suggestions for subsequent development are proposed.

Keywords: Machine learning, phosphors, materials genome initiative

INTRODUCTION

Data-driven machine learning (ML) has become the frontier of materials science since the Materials Genome Initiative (MGI) for Global Competitiveness program was launched^[1-4]. After several years of rapid development, ML has yielded promising achievements in novel materials development^[5-7]. Hart *et al.* reviewed the progress of ML-assisted alloy research and summarized the typical applications of ML in amorphous, high-entropy and shape memory alloys, magnetic materials and superalloys^[8]. Liu *et al.*



© The Author(s) 2022. **Open Access** This article is licensed under a Creative Commons Attribution 4.0 International License (<https://creativecommons.org/licenses/by/4.0/>), which permits unrestricted use, sharing, adaptation, distribution and reproduction in any medium or format, for any purpose, even commercially, as long as you give appropriate credit to the original author(s) and the source, provide a link to the Creative Commons license, and indicate if changes were made.



www.jmijournal.com

reviewed the recent progress and prospects of ML in assisting the design and discovery of rechargeable battery materials^[9]. Wang *et al.* examined the progress of ML in thermoelectric materials and discussed possible strategies for using small databases to facilitate the development of materials science^[10]. Lookman *et al.* summarized the application of active learning in accelerating the exploration and discovery of new materials by reviewing adaptive experimental sampling and Bayesian optimization methods^[11].

Inorganic phosphors are one of the most important components of light-emitting diode (LED)-based lighting sources^[12,13]. Currently, the chip technology used to excite phosphors has matured and the properties of inorganic phosphors directly affect the performance of the LED device. The phosphors used in LEDs should consider the basic criteria of high quantum efficiency, high thermal stability and appropriate emission wavelength^[14-16]. So far, significant effort has been devoted to the design and discovery of novel LED phosphors for solid-state lighting^[17-19]. As for inorganic phosphors, more than 50% of the elements in the periodic table can form luminescent material matrices, resulting in a huge optimization space. In the past, trial-and-error optimization strategies have been the primary approach to the development of luminescent materials, which can be divided into two categories, namely, new luminescent materials can be discovered by doping the luminescent centers^[20-23], taking the natural mineral structure (such as garnet, perovskite, spinel and so on) as the matrix material and novel luminescent materials development through ion substitution strategies based on already known luminescent materials^[24-29]. Due to the huge search space, traditional trial-and-error experiments suffer from the disadvantages of low efficiency and high cost. The emergence of ML provides opportunities for the efficient development of new inorganic phosphors and some researchers have started to apply ML to the development of inorganic phosphors. **Table 1** lists all the recent work on ML for inorganic phosphors that we are aware of.

In this mini review, we summarize the recent advances in the application of ML for inorganic phosphors, focusing on the ML methods used in these works and the results generated. According to the applied methods, we divide it into two aspects, namely, material properties prediction and optimization based on iterative experiments and provide an outlook for their future directions.

ML-ASSISTED INORGANIC PHOSPHOR DISCOVERY

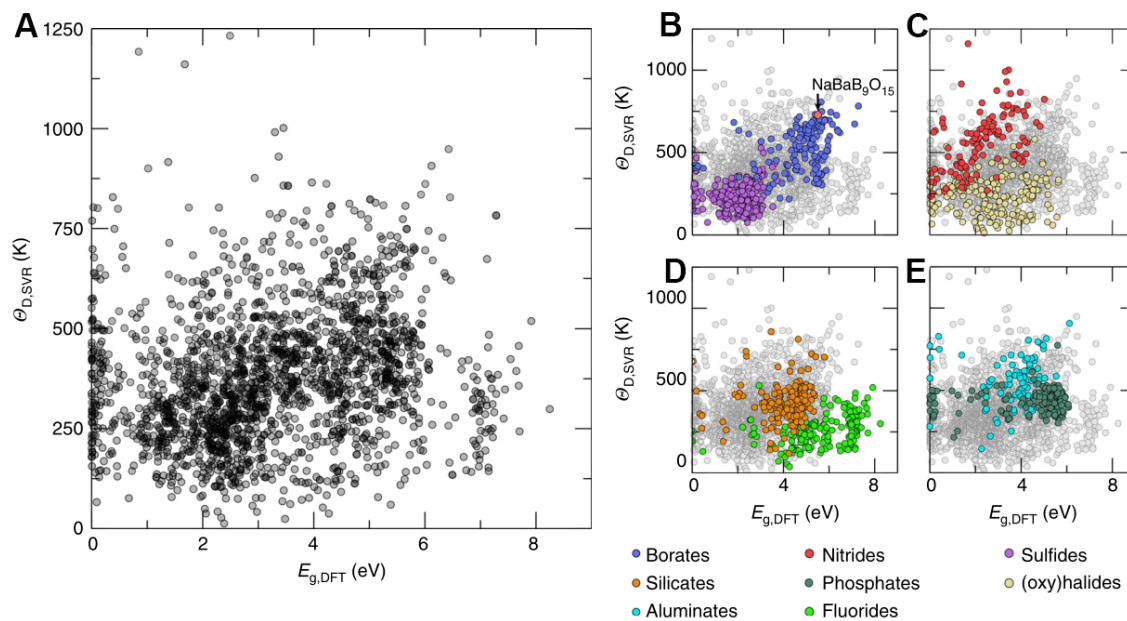
Material properties prediction

Accurately predicting materials properties can help us rapidly identify materials that meet performance requirements and reduce the cost of experiments. For phosphors, the key properties include emission wavelength, thermal stability and quantum efficiency. It is known that a wide band gap of the matrix is crucial to the luminescence efficiency of a phosphor and when the bandwidth is small, the 5d orbitals in the excited state may be close enough to the conduction band of the matrix, leading to temperature-induced photoionization or charge transfer. In contrast, the structural rigidity of a phosphor is closely related to its thermal stability and a higher structural rigidity can effectively suppress the nonradiative transitions, which in turn gives rise to a phosphor with high efficiency. However, it is often difficult to identify compounds that are more structurally rigid than others^[40]. A more tractable method for determining structural rigidity is to evaluate the Debye temperature of the material^[41].

To rapidly predict the Debye temperature of inorganic materials, Zhuo *et al.* constructed a Debye temperature prediction model by support vector regression (SVR) with 150 material features and a 2610 training set calculated by DFT ($R^2 = 0.89$)^[30]. By cross-referencing the DFT band gap information in the Materials Project and the Pearson Crystal Database (PCD), 2071 compounds were screened out for Debye temperature prediction. Finally, the NaBaB₆O₁₅ matrix was identified by the comprehensive screening of the predicted Debye temperature and the bandwidth obtained from DFT calculations [Figure 1]. The

Table 1. Overview of ML applications for inorganic phosphors

Year	Description	References
Material properties prediction		
2018	Predicting Debye temperature of inorganic matrices	[30]
2019	Predicting excitation wavelength of phosphors	[31]
2020	Predicting 5d-level centroid shift of Ce ³⁺ -doped inorganic phosphors	[32]
2020	Predicting thermal quenching temperature in Eu ³⁺ -substituted oxide phosphors	[33]
2021	Predicting band gap, excitation and emission energies for Eu ²⁺ -activated phosphors	[34]
Material properties optimization based on iterative experiments		
2018	Optimizing luminous intensity of REOF:xEu ³⁺	[35]
2019	Optimizing luminous intensity of REOF:xCe, yTb (RE = Gd, La or Lu)	[36]
2020	Optimizing luminous intensity of LuOF:Yb/Er/Mn/K/Li	[37]
2021	Optimizing color temperature and color rendering index of white phosphors	[38]
2022	Optimizing thermal stability of cyan-green garnet:Ce phosphors	[39]

**Figure 1.** (A) Phosphors predicted by Debye temperature and bandwidth. (B) Borates and sulfides; (C) nitrides and (oxy)halides; (D) silicates and fluorides and (E) aluminates and phosphates. Reprinted with permission from Zhuo et al.^[30], copyright 2019, Nature Press.

Eu²⁺-doped NaBaB₉O₁₅ phosphor was prepared and characterized by high efficiency and excellent thermal stability.

The Debye temperature is an intrinsic factor that affects thermal stability. In order to predict thermal stability more intuitively, the quenching temperature (T₅₀), which is commonly used to indicate thermal stability, can be used as the prediction goal. In order to find oxide phosphors with excellent thermal stability, Zhuo et al.^[33] trained the SVR thermal quenching temperature (T₅₀) model with 134 experimental data as the training set. In the training process, 178 initial features were constructed and 51 optimal features were obtained by the recursive feature elimination method with R² = 0.71 [Figure 2A]. The trained model was used for the T₅₀ prediction of 1331 oxides in the PCD. Based on the prediction results, the phosphors

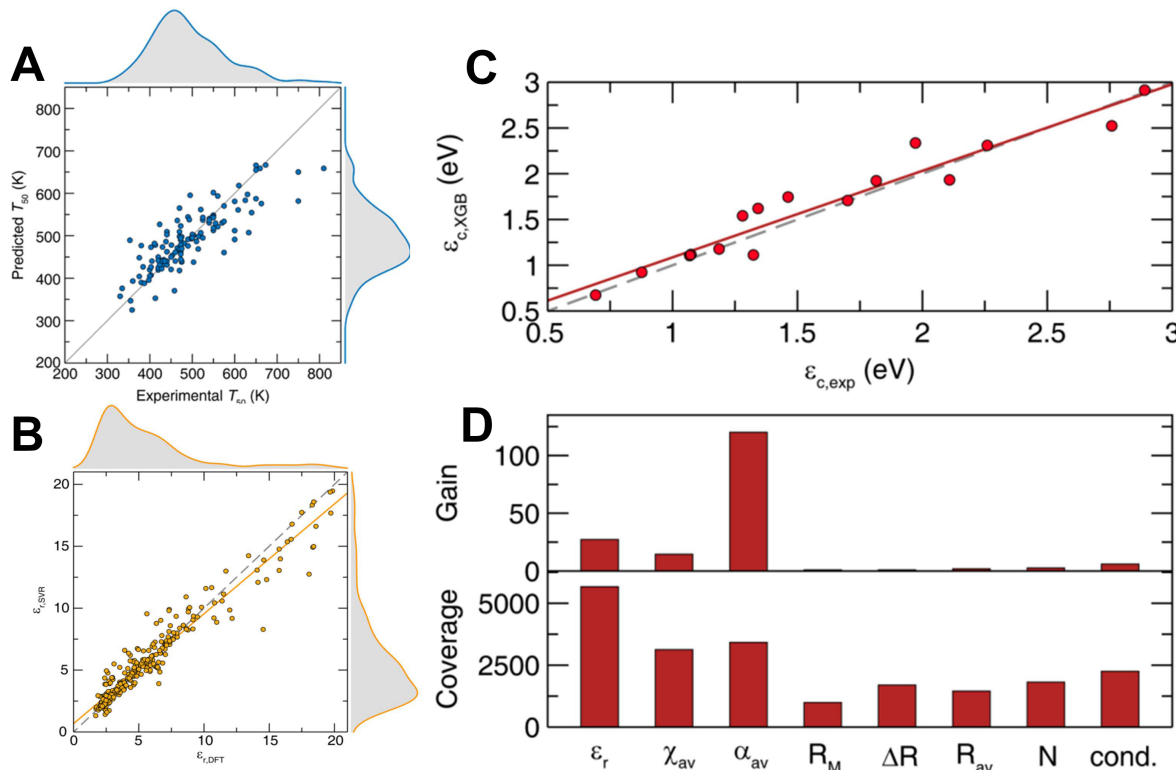


Figure 2. (A) T50 model performance. Reprinted with permission from Zhuo et al.^[33], copyright 2020, American Chemical Society. (B) Predicted relative permittivity. (C) XGB model predicted centroid shift against experimentally measured centroid shift. (D) Feature importance of XGB model in terms of gain and coverage. Reprinted with permission from Zhuo et al.^[32], copyright 2020, AIP Publishing.

Eu^{2+} -doped $\text{Sr}_2\text{ScO}_3\text{F}$, $\text{Cs}_2\text{MgSi}_5\text{O}_{12}$, $\text{Ba}_2\text{P}_2\text{O}_7$, $\text{LiBaB}_9\text{O}_{15}$ and $\text{Y}_3\text{Al}_5\text{O}_{12}$ were prepared and characterized. Due to the limited training data, the model does not perform very well compared to other models with rich data. Nevertheless, it can help us to identify the possibility of thermal stability of a specific structure and enable the rapid development of new materials.

In addition, the excitation and emission wavelengths of phosphors affect their application scenarios. The 5d-level centroid shift of rare earth ions can help us better understand their luminescence properties. Phosphors with a larger centroid shift tend to have longer emission wavelengths and the luminescence color can be estimated using the centroid shift. In order to predict the centroid shift of phosphors, Zhuo et al. constructed the SVR relative permittivity prediction model based on 2832 relative permittivity data from the Materials Project with 98 features, including 17 distinct compositional variables describing elemental properties and 13 structural descriptors related to variables [Figure 2B]^[32]. The relative permittivity of over 27,000 compounds in the PCD was predicted. The XGB model was then trained based on 160 data extracted from the literature with nine features, such as relative permittivity predicted by the SVR model and average cation electronegativity, average anion polarizability, average cation electronegativity, and so on. The model was validated with an accuracy of $R^2 = 0.9$ on the hold-out 10% of the training set [Figure 2C]. Feature importance of the XGB model was evaluated based on gain and coverage matrix. The results show that the average anion polarizability, relative permittivity and average cation electronegativity are the most essential features related to the centroid shift [Figure 2D].

Additionally, the 18 prediction models of the excitation band edge wavelength (EBEW), peak emission wavelength (PEW) and band gap were trained by Park *et al.* based on 91 experimental data extracted from the literature with 29 features, such as elemental and structural features, respectively. Four EBEW ML models, seven PEW ML models and six Eg ML models were screened out by the screening metrics $R^2 > 0.6$, $MSE < 0.02$ and overfitting index $(R^2_{\text{test}}/R^2_{\text{training}}) > 0.77$, respectively^[34]. Barai *et al.* trained excitation wavelength least absolute shrinkage and selection operator (LASSO) and artificial neural network (ANN) models based on 48 phosphors with a known host containing three elements^[31]. There were 83 features used to train the model, covering 15 properties of each atom in the compound, five calculated values and three standard physical constants related to photon behavior. The accuracy R^2 of the trained LASSO and ANN models on the training set reached 0.99 and 0.99, respectively. These two works trained the prediction models but did not validate them in practice and their generalization ability for wavelength prediction is therefore unclear.

Material properties optimization based on iterative experiments

ML techniques are based on materials data. However, the current data available for phosphors are typically few and sparse, mostly in the range of tens to hundreds, and the accuracy of predictions is, therefore, usually low. Active learning and heuristic algorithms are two commonly used methods for materials optimization [Figure 3]. Active learning is applicable to ML models built on materials data with high dimensionality, small size, high noise and uneven distribution, which usually exhibit low prediction accuracy, poor generalization ability and high uncertainty. The heuristic optimization algorithm achieves efficient global optimization of materials by searching for a locally optimal solution. It can be used for the exploration of new materials with a huge search space.

Active learning

Active learning strategies can be used to effectively improve the model prediction accuracy through experimental validation and data feedback iterations. Active learning establishes the utility function (selector) that balances the predicted value with the uncertainty of the constructed model. The most commonly used selectors are expected improvement (EI)^[42,43], probability of improvement (PI)^[44] and upper confidence bounds (UCB)^[45-47], which can be expressed by Equations (1)-(3), respectively:

$$PI(x) = P(f(x)) \geq P(f(x^*)) = \Phi\left(\frac{\mu(x) - f(x^*)}{\sigma(x)}\right) \quad (1)$$

$$EI(x) = (\mu(x) - f(x^*))\Phi(Z) + \sigma(x)\phi(Z) \quad (2)$$

$$UCB(x) = \mu(x) + \kappa\sigma(x) \quad (3)$$

where $Z = (\mu(x) - f(x^*)) / \sigma(x)$, $\Phi(Z)$ and $\phi(Z)$ are the cumulative distribution functions and standard normal density, respectively, $\mu(x)$ denotes the mean of the predictions, $\sigma(x)$ is the standard deviation of the predictions, $f(x^*)$ is the maximum target value in the training set and κ is a hyperparameter (a κ value of 1.96 represents a 95% confidence level). The κ value can be set according to the requirements, through which exploration (the uncertainty in the model is large) and exploitation (where the model prediction is high) can be balanced.

In order to optimize the color temperature (CCT) and color rendering index (CRI) of the (TDMP)Pb(Br_xCl_{1-x})₄:yMn phosphor system, Yuan *et al.* trained CCT and CRI polynomial regression ML

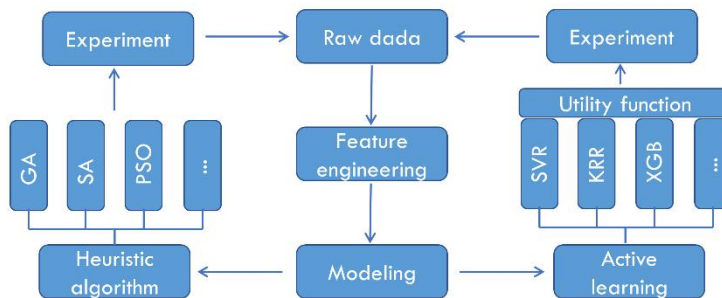


Figure 3. Strategies for materials optimization.

models based on 55 sets of experimental data, with the material chemical compositions as features^[38]. During the iteration, the (x, y) of randomly selected 15 CCTs at 3000–7000 K were determined by the CCT model and then the maximum CRI corresponding to each CCT was determined by the CRI model. The (x, y) corresponding to the maximum CRI was selected for synthesis. Under the guidance of the model, the authors obtained a series of white phosphors with an ultrahigh CRI. To select the candidates for the experiment, the authors made their choice based on predicted values and the results showed that this selection strategy provides an effective guide for the optimization of CCT and CRI.

Recently, our group has applied active learning methods to the development of Ce-doped garnet phosphors^[39]. We constructed a wavelength model with seven features and a thermal stability (T₆₀) model with six features based on 70 data instances obtained from literature through the process of feature and model selection and model evaluation. In this process, the Pearson correlation coefficient was used to remove highly linearly correlated and key features and optimal ML model combinations affecting the wavelength and thermal stability were obtained by a wrapper feature selection method. Subsequently, the wavelength model was used to screen out the phosphors in the wavelength range of 480–510 nm in the constructed 171,636 compounds. The T₆₀ model was then used in combination with an efficient global optimization strategy to obtain the candidate experimental compounds [Figure 4]. EI was used as the selector. The cyan-green phosphor ($\text{Lu}_{1.5}\text{Sr}_{1.5}\text{Al}_{3.5}\text{Si}_{1.5}\text{O}_{12}$:Ce) with excellent thermal stability was obtained by only five iterations. $\text{Lu}_{1.5}\text{Sr}_{1.5}\text{Al}_{3.5}\text{Si}_{1.5}\text{O}_{12}$:Ce performs the best with excellent thermal stability ($\geq 60\%$ emission intensity retained at 640 K, Figure 4E) and exhibits emission peaks of ~ 505 nm [Figure 4D].

Heuristic algorithm

Another category of optimization methods is heuristic algorithm optimization, including genetic algorithms (GAs), simulated annealing algorithms and particle swarm optimization (PSO). Global optimization is achieved by continuously searching for local optimal solutions in a finite materials feature space.

Lv *et al.* optimized the luminescence intensity of REOF:xEu³⁺ down-conversion and LuOF:Yb/Er/Mn/K/Li up-conversion phosphors with a heuristic GA^[35,37]. In the optimization process, the first-generation phosphors were prepared empirically as the initial population, the composition of prepared phosphors was mapped into binary codes simultaneously and then the second-generation phosphors were obtained by selection, crossover and mutation operations and cycled in this way. After optimization, the third generation LuOF:Yb/Er/Mn/K/Li phosphor showed the best luminescence intensity, possessing stronger brightness (4.91 times), higher relative quantum yield (6.40 times) and stronger depth of tissue penetration (5 mm). The final brightness of REOF:xEu³⁺ was improved by 141%. In addition, they compared the performance of four HAs for the luminescence intensity optimization of REOF:xCe, yTb (RE = Gd, La or

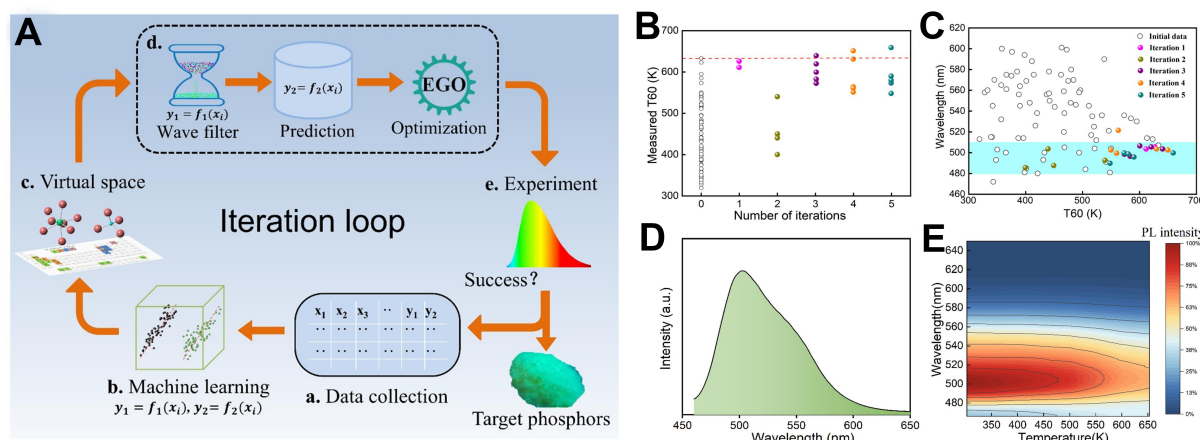


Figure 4. (A) Iteration loop of phosphor design accelerated by ML. The design loop includes data collection, ML, search space, adaptive experimental design, experiment and measurement. (B) Experimental T60 as a function of iteration number. (C) Spatial distribution of experimental wavelength and experimental T60. (D) Emission spectra and (E) temperature-dependent emission spectra of $\text{Lu}_{1.5}\text{Sr}_{1.5}\text{Al}_{3.5}\text{Si}_{1.5}\text{O}_{12}:\text{Ce}$. Reprinted with permission from Jiang et al.^[39], copyright 2022, American Chemical Society.

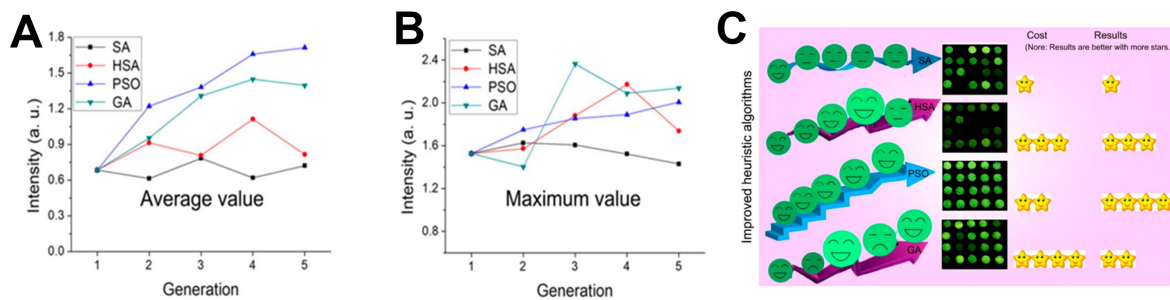
Lu) phosphors, including SA, improved annealing with a harmony search algorithm (HSA), PSO and GA, as shown in Figure 5. The results show that all algorithms present good guidance for the synthesis of luminescent powders. The global searching ability of the HSA was significantly improved and obtained better phosphors than the SA. The PSO algorithm obtained the best results with increased generation but required a higher experimental cost. The GA could find the acceptable phosphor in a shorter time and cost^[36].

CONCLUSION AND PROSPECTS

Relevant studies have shown that ML can effectively achieve phosphor properties prediction and accelerate the development of novel inorganic phosphors. ML will bring greater potential when more researchers put in the effort. Simultaneously, compared to other material fields, the application of ML in inorganic luminescent materials is relatively few and still in its infancy. Based on current research, we propose the following suggestions for the future application of ML in inorganic phosphors:

Physical feature construction and interpretable models

To interpret the ML model of inorganic phosphors will bring more inspiration to materials design. At this stage, the ML of phosphors is mainly based on the black-box model and the model features are mainly elemental features and chemical composition. It is not available to understand the physical meaning behind the models. More effective descriptors with physical meaning are expected to be explored. In the prediction of centroid shift, Zhuo *et al.* trained the XGB model by nine features, such as relative permittivity, which is beneficial for interpreting and predicting the luminescence properties and thermal quenching behaviors for Ce^{3+} -doped phosphors^[32]. Song *et al.* set up a novel structural indicator to characterize the crystal-field splitting of Ce^{3+} in garnet-type compounds^[48]. It has a simple form, which is the sum of oxygen coordinates multiplied by the cell parameter. They also introduced a structural descriptor, the tolerance factor, for the prediction and systematic description of the phase stability with the garnet structure^[49]. These structural descriptors are promising for the ML of Ce^{3+} -doped inorganic phosphors. Therefore, the construction of physically meaningful features, and thus interpretable ML models, are of great importance to the development of luminescent materials.



Database construction

After a long period of development, researchers have established the Inorganic Crystal Structure Database (ICSD), Pearson Crystal Database (PCD) and Materials Project (MP) for the field of inorganic materials and these databases have provided great convenience for ML. However, there is still a lack of a database of luminescent materials, as well as their composition-structure-property relationships. At present, collecting data from the published literature is an effective method. This helps to make full use of the existing literature resources and reduce costs. Encouraging the unification of testing methods and testing techniques would contribute to the construction of a database suitable for ML.

Multi-objective optimization

The application of materials requires the balance of multiple properties, such as the main properties of inorganic phosphors, including wavelength, thermal stability, quantum efficiency, and so on. Achieving multi-objective collaborative optimization is an important problem faced in materials applications. Therefore, it is essential to conduct research on the application of ML multi-objective optimization in inorganic luminescent materials. Considering the problem of a small dataset of luminescent materials, the combination of multi-objective optimization and an active learning approach is still an effective method. Consequently, the utility function applicable to the multi-objective optimization problem also needs to be developed.

DECLARATIONS

Authors' contributions

Planned and designed: Su Y, Jiang L

All authors participated in the writing or revising of the manuscript.

All authors have given approval to the final version of the manuscript.

Availability of data and materials

Not applicable.

Financial support and sponsorship

This work was financially supported by the National Key Research and Development Program of China (2021YFB3501501) and Guangdong Province Key Area R & D Program (2019B010940001).

Conflicts of interest

All authors declared that there are no conflicts of interest.

Ethical approval and consent to participate

Not applicable.

Consent for publication

Not applicable.

Copyright

© The Author(s) 2022.

REFERENCES

1. White House Office of Science and Technology Policy. Materials genome initiative for global competitiveness. Available from: https://obamawhitehouse.archives.gov/sites/default/files/microsites/ostp/materials_genome_initiative-final.pdf [Last accessed on 13 Sep 2022].
2. Su Y, Fu H, Bai Y, Jiang X, Xie J. Progress in materials genome engineering in China. *Acta Metallurgica Sinica* 2020;56:1313-23. [DOI](#)
3. Xie J, Su Y, Xue D, Jiang X, Fu H, Huang H. Machine learning for materials research and development. *Acta Metallurgica Sinica* 2021;57:1343-61. [DOI](#)
4. Xie J, Su Y, Zhang D, Feng Q. A vision of materials genome engineering in China. *Engineering* 2022;10:10-2. [DOI](#)
5. Wen C, Zhang Y, Wang C, et al. Machine learning assisted design of high entropy alloys with desired property. *Acta Materialia* 2019;170:109-17. [DOI](#)
6. Liu P, Huang H, Antonov S, et al. Machine learning assisted design of γ' -strengthened Co-base superalloys with multi-performance optimization. *npj Comput Mater* 2020;6. [DOI](#)
7. Zhang Y, Wen C, Wang C, et al. Phase prediction in high entropy alloys with a rational selection of materials descriptors and machine learning models. *Acta Materialia* 2020;185:528-39. [DOI](#)
8. Hart GLW, Mueller T, Toher C, Curtarolo S. Machine learning for alloys. *Nat Rev Mater* 2021;6:730-55. [DOI](#)
9. Liu Y, Guo B, Zou X, Li Y, Shi S. Machine learning assisted materials design and discovery for rechargeable batteries. *Energy Stor Mater* 2020;31:434-50. [DOI](#)
10. Wang T, Zhang C, Snoussi H, Zhang G. Machine learning approaches for thermoelectric materials research. *Adv Funct Mater* 2020;30:1906041. [DOI](#)
11. Lookman T, Balachandran PV, Xue D, Yuan R. Active learning in materials science with emphasis on adaptive sampling using uncertainties for targeted design. *npj Comput Mater* 2019;5. [DOI](#)
12. Xia Z, Liu Q. Progress in discovery and structural design of color conversion phosphors for LEDs. *Progr Mater Sci* 2016;84:59-117. [DOI](#)
13. Xia Z, Meijerink A. Ce³⁺-doped garnet phosphors: composition modification, luminescence properties and applications. *Chem Soc Rev* 2017;46:275-99. [DOI](#) [PubMed](#)
14. Li S, Wang L, Hirosaki N, Xie R. Color conversion materials for high - brightness laser - driven solid - state lighting. *Laser & Phot Revi* 2018;12:1800173. [DOI](#)
15. Wang Y, Ding J, Wang Y, et al. Structural design of new Ce³⁺/Eu²⁺ -doped or co-doped phosphors with excellent thermal stabilities for WLEDs. *J Mater Chem C* 2019;7:1792-820. [DOI](#)
16. Tian J, Zhuang W. Thermal stability of nitride phosphors for light-emitting diodes. *Inorg Chem Front* 2021;8:4933-54. [DOI](#)
17. He M, Jia J, Zhao J, Qiao X, Du J, Fan X. Glass-ceramic phosphors for solid state lighting: a review. *Ceram Int* 2021;47:2963-80. [DOI](#)
18. Dang P, Wang W, Lian H, Li G, Lin J. How to obtain anti-thermal-quenching inorganic luminescent materials for light-emitting diode applications. *Adv Opt Mater* 2022;10:2102287. [DOI](#)
19. Zhao F, Song Z, Liu Q. Advances in chromium-activated phosphors for near-infrared light sources. *Laser & Photonics Rev* ;2022:2200380. [DOI](#)
20. Xiahou J, Zhu Q, Zhu L, Li S, Li J. Local structure Regulation in near-infrared persistent phosphor of ZnGa₂O₄:Cr³⁺ to fabricate natural-light rechargeable optical thermometer. *ACS Appl Electron Mater* 2021;3:3789-803. [DOI](#)
21. Jiang L, Jiang X, Xie J, Zheng T, Lv G, Su Y. Structural induced tunable NIR luminescence of (Y,Lu)₃(Mg,Al)₂(Al,Si)₃O₁₂:Cr³⁺ phosphors. *J Lumin* 2022;247:118911. [DOI](#)
22. Liu T, Cai H, Mao N, Song Z, Liu Q. Efficient near-infrared pyroxene phosphor LiInGe₂O₆:Cr³⁺ for NIR spectroscopy application. *J Am Ceram Soc* 2021;104:4577-84. [DOI](#)
23. Zeng H, Zhou T, Wang L, Xie R. Two-Site Occupation for exploring ultra-broadband near-infrared phosphor - double-perovskite La₂MgZrO₆:Cr³⁺. *Chem Mater* 2019;31:5245-53. [DOI](#)
24. He C, Ji H, Huang Z, et al. Red-shifted emission in Y₃MgSiAl₃O₁₂:Ce³⁺ garnet phosphor for blue light-pumped white light-emitting diodes. *J Phys Chem C* 2018;122:15659-65. [DOI](#)
25. Yan Y, Shang M, Huang S, et al. Photoluminescence properties of AScSi₂O₆:Cr³⁺ (A = Na and Li) phosphors with high efficiency and

- thermal stability for near-infrared phosphor-converted light-emitting diode light sources. *ACS Appl Mater Interfaces* 2022;14:8179-90. [DOI](#) [PubMed](#)
- 26. Wang Y, Wang Z, Wei G, et al. Ultra-broadband and high efficiency near-infrared $\text{Gd}_3\text{ZnGa}_5\text{-}2\text{GeO}_{12}\text{:Cr}^{3+}$ ($x = 0\text{-}2.0$) garnet phosphors via crystal field engineering. *Chem Eng J* 2022;437:135346. [DOI](#)
 - 27. Zhang L, Wang D, Hao Z, et al. Cr^{3+} -doped broadband NIR garnet phosphor with enhanced luminescence and its application in NIR spectroscopy. *Adv Optical Mater* 2019;7:1900185. [DOI](#)
 - 28. Jiang L, Zhang X, Tang H, et al. A $\text{Mg}^{2+}\text{-Ge}^{4+}$ substituting strategy for optimizing color rendering index and luminescence of YAG: Ce^{3+} phosphors for white LEDs. *Mater Res Bull* 2018;98:180-6. [DOI](#)
 - 29. Jiang L, Jiang X, Xie J, et al. Ultra-broadband near-infrared $\text{Gd}^3\text{MgScGa}^2\text{SiO}_{12}\text{:Cr}$, Yb phosphors: photoluminescence properties and LED applications. *J Alloys Comp* 2022;920:165912. [DOI](#)
 - 30. Zhuo Y, Mansouri Tehrani A, Oliynyk AO, Duke AC, Brgoch J. Identifying an efficient, thermally robust inorganic phosphor host via machine learning. *Nat Commun* 2018;9:4377. [DOI](#) [PubMed](#) [PMC](#)
 - 31. Barai VL, Dhoble S. Prediction of excitation wavelength of phosphors by using machine learning model. *J Lumin* 2019;208:437-42. [DOI](#)
 - 32. Zhuo Y, Hariyani S, You S, Dorenbos P, Brgoch J. Machine learning 5d-level centroid shift of Ce^{3+} inorganic phosphors. *J Appl Phys* 2020;128:013104. [DOI](#)
 - 33. Zhuo Y, Hariyani S, Armijo E, Abolade Lawson Z, Brgoch J. Evaluating thermal quenching temperature in Eu^{3+} -substituted oxide phosphors via machine learning. *ACS Appl Mater Interfaces* 2020;12:5244-50. [DOI](#) [PubMed](#)
 - 34. Park C, Lee J, Kim M, et al. A data-driven approach to predicting band gap, excitation, and emission energies for Eu^{2+} -activated phosphors. *Inorg Chem Front* 2021;8:4610-24. [DOI](#)
 - 35. Lv R, Xiao L, Jiang X, Feng M, Yang F, Tian J. Optimization of red luminescent intensity in Eu^{3+} -doped lanthanide phosphors using genetic algorithm. *ACS Biomater Sci Eng* 2018;4:4378-84. [DOI](#) [PubMed](#)
 - 36. Lv R, Xiao L, Wang Y, Yang F, Tian J, Lin J. Searching for the optimized luminescent lanthanide phosphor using heuristic algorithms. *Inorg Chem* 2019;58:6458-66. [DOI](#) [PubMed](#)
 - 37. Yang F, Wang Y, Jiang X, Lin B, Lv R. Optimized multimetal sensitized phosphor for enhanced red up-conversion luminescence by machine learning. *ACS Comb Sci* 2020;22:285-96. [DOI](#) [PubMed](#)
 - 38. Yuan H, Qi L, Paris M, et al. Machine learning guided design of single-phase hybrid lead halide white phosphors. *Adv Sci (Weinh)* 2021;8:e2101407. [DOI](#) [PubMed](#) [PMC](#)
 - 39. Jiang L, Jiang X, Zhang Y, et al. Multiobjective machine learning-assisted discovery of a novel cyan-green garnet: Ce phosphors with excellent thermal stability. *ACS Appl Mater Interfaces* 2022;14:15426-36. [DOI](#) [PubMed](#)
 - 40. Lin Y, Bettinelli M, Sharma SK, et al. Unraveling the impact of different thermal quenching routes on the luminescence efficiency of the $\text{Y}_3\text{Al}_5\text{O}_{12}\text{:Ce}^{3+}$ phosphor for white light emitting diodes. *J Mater Chem C* 2020;8:14015-27. [DOI](#)
 - 41. Hermus M, Brgoch J. Phosphors by design: approaches toward the development of advanced luminescent materials. *Interface magazine* 2015;24:55-9. [DOI](#)
 - 42. Kushner H J. A new method of locating the maximum of an arbitrary multipeak curve in the presence of noise. *J Basic Eng* 1964;86:97-106. [DOI](#)
 - 43. Carr SF, Garnett R, Lo CS. Accelerating the search for global minima on potential energy surfaces using machine learning. *J Chem Phys* 2016;145:154106. [DOI](#) [PubMed](#)
 - 44. de Jong M, Chen W, Notestine R, et al. A statistical learning framework for materials science: application to elastic moduli of k-nary inorganic polycrystalline compounds. *Sci Rep* 2016;6:34256. [DOI](#) [PubMed](#) [PMC](#)
 - 45. Cox DD, John S. A statistical method for global optimization. *IEEE Int Conf Syst, Man, Cybern* 1992;1241-46. [DOI](#)
 - 46. Cox DD, John S. A statistical method for global optimization. *IEEE Int Conf Syst, Man, Cybern* 1997;315-29. [DOI](#)
 - 47. Burger B, Maffettone PM, Gusev VV, et al. A mobile robotic chemist. *Nature* 2020;583:237-41. [DOI](#) [PubMed](#)
 - 48. Song Z, Liu Q. Structural indicator to characterize the crystal-field splitting of Ce^{3+} in garnets. *J Phys Chem C* 2020;124:870-3. [DOI](#)
 - 49. Song Z, Zhou D, Liu Q. Tolerance factor and phase stability of the garnet structure. *Acta Crystallogr C Struct Chem* 2019;75:1353-8. [DOI](#) [PubMed](#)